Wiley
Stem Cells International
Volume 2025, Article ID 3010753, 13 pages
https://doi.org/10.1155/sci/3010753

WILEY

Research Article

Optimizing the Banking and Releasing Strategies of Clinical-Grade HLA-Homozygous Human iPSCs for Regenerative Medicine

Qianping Zhang,[1] **Lijuan Cui**,[1] **Ying Jia**,[1] **Xiaohui Shi**,[1] **Jinmei Zhang**,[1] **Li Zhang**,[1] **Zhihui Liu**,[1] **Yun Zhang**,[2] **Huizhuan Fu**,[2] **Qi Qi**,[2] **Quan Chen**,[3] **Wei Du**,[1] **and Yu Zhang**[1,2]

[1]*Tianjin Key Laboratory for Blood Cell Therapy Technology, Union Stem Cell Gene Engineering Co., Ltd., Tianjin, China*
[2]*VCANBIO Cell and Gene Engineering Corp., Ltd., Tianjin, China*
[3]*College of Life Sciences, Nankai University, Tianjin, China*

Correspondence should be addressed to Wei Du; duweixhgxb@vcanbio.com and Yu Zhang; zhangyu@vcanbio.com

Received 7 March 2025; Revised 18 September 2025; Accepted 26 September 2025

Academic Editor: Annamaria Sapuppo

Since their initial generation, induced pluripotent stem cells (iPSCs) have attracted considerable attention and undergone rapid development. iPSC-derived cell therapies show great promise in the field of regenerative medicine. However, their clinical translation faces two major challenges: the limited availability of good manufacturing practice (GMP)-compliant human iPSC (hiPSC) lines, and the high costs and prolonged timelines associated with autologous hiPSC-based therapies. Allogeneic therapies based on rigorously quality-controlled, GMP-compliant, human leukocyte antigen (HLA)-homozygous hiPSCs thus represent a promising alternative. In this study, we established and validated a GMP-compliant platform for iPSCs production, complete with a comprehensive set of standard operating procedures (SOPs) and recommended release criteria for the iPSC master cell bank (MCB). Using frozen umbilical cord blood (UCB) from donors with high-frequency HLA homozygosity as starting material, we generated five monoclonal iPSC MCB lines and performed full release testing. Among the five iPSC lines, three demonstrated high post-thaw survival rates, met all release criteria, and exhibited strong potential for multilineage differentiation and clinical application in cell therapy.

Keywords: cell therapy; clinical translation; GMP production; induced pluripotent stem cells; umbilical cord blood

1. Introduction

The generation of induced pluripotent stem cells (iPSCs) was first reported by Shinya Yamanaka's group in 2006 [1], followed by the derivation of human iPSCs (hiPSCs) in 2007 by Shinya Yamanaka's group [2] and James Thomson's group [3]. Since these landmark advances, iPSCs have revolutionized regenerative medicine by offering a renewable source of patient-specific cells for use in disease modeling, drug screening, and cell therapy [4, 5]. Notable clinical advancements have underscored this potential: in 2024, Deng's group reported the first successful transplantation of hiPSC-derived pancreatic islets into a patient with type 1 diabetes, who achieved complete insulin independence within 75 days [6]. The same year, a groundbreaking study demonstrated the first successful transplantation of hiPSC-derived corneal tissue into patients with corneal limbal stem cell deficiency, leading to substantial visual recovery [7]. Despite these promising developments, the clinical translation of iPSC-based therapies continues to face significant obstacles, including immune rejection, concerns regarding genetic safety, high manufacturing costs, and limited scalability [8–10]. To overcome these challenges, the development of clinical-grade allogeneic iPSC banks from human leukocyte antigen (HLA)-homozygous

donors with minimal mutational burden has emerged as a highly promising strategy solution.

Umbilical cord blood (UCB) represents an ideal starting material for the generation of clinical-grade iPSCs due to a number of advantageous characteristics. Cord blood mononuclear cells (CBMCs), which encompass hematopoietic stem cells, mesenchymal stromal cells, and endothelial progenitor cells, demonstrate high proliferative capacity and low immunogenicity [11]. In contrast to adult somatic cells, CBMCs exhibit limited exposure to environmental stressors and accumulated genetic mutations, thereby providing a high-quality source for reprograming [12, 13]. In addition, UCB collection is noninvasive, ethically straightforward, and can be readily accessed via public cord blood banks, facilitating a sustainable cellular source for large-scale iPSCs production [14].

Notably, HLA matching plays a critical role in reducing immune rejection in cell transplantation [15]. CBMCs obtained from HLA-homozygous donors possess particular advantages. Their unique immunogenic profile, characterized by reduced HLA antigen expression and a lower propensity for graft-versus-host disease, makes them especially appropriate for allogeneic iPSC-based cell therapy applications [16].

Recently, significant progress has been made by multiple countries in establishing good manufacturing practice (GMP)-compliant HLA-homozygous iPSC banks, including Japan [17], South Korea [18], Australia [19], the Netherlands [20], Spain [21], and Saudi Arabia [22]. Brazil has also established a clinical-grade iPSC bank [23]. The primary objective of these initiatives is to address the persistent challenge of donor shortage in cell therapy. Conventional stem cell transplantation depends on the availability of HLA-matched donors, who are often scarce, particularly for patients carrying rare HLA haplotypes [24]. HLA-homozygous iPSC banks offer a promising solution by providing a sustainable and readily accessible source of "off-the-shelf" cell products with broad population compatibility. Therefore, the development of GMP-compliant HLA-homozygous iPSC banks not only simplifies therapeutic workflows but also greatly enhances the accessibility and efficacy of iPSC-derived therapies, representing a major advance in regenerative medicine.

In this study, we reported the development of a GMP-compliant iPSCs production platform and the recommended release criteria for iPSC master cell bank (MCB). Using frozen UCB from high-frequency HLA-homozygous donors as starting material, we established five monoclonal iPSC MCB lines and conducted comprehensive release testing. Among these, three lines with high post-thaw survival rates met all release criteria and exhibited robust potential for multilineage differentiation and clinical application in cell therapy. Our GMP-compliant platform lays a foundation for standardized and cost-effective manufacturing of iPSC-based therapies, thereby broadening the reach of regenerative medicine to diverse patient populations.

2. Materials and Methods

2.1. Donor Screening. Documents of cord blood donors with target HLA typing were confidentially and thoroughly reviewed to verify the completeness, including but not limited to informed consents, health questionnaires, sterility test reports, and human virus screening results. All UCB-related data were anonymized to ensure donor privacy. The informed consent forms obtained from UCB donors explicitly covered the use of donated samples for iPSCs derivation and potential future clinical applications in regenerative medicine. The consent procedure, which was reviewed and approved by the Ethics Committee of the Institute of Hematology and Blood Diseases Hospital (Approval Number: YW2018001-EC-1), guaranteed that participation was voluntary and would not affect the donor's own medical care. Donors were provided with a detailed information sheet, and the original signed consent forms are retained by our institution. Male donors with blood type O were given priority for iPSCs banking. Candidates passing initial documentation review underwent reconfirmation of HLA typing to validate homozygosity across five key loci and consistency with donor records. Short tandem repeat (STR) profiling with 21-allele markers was additionally performed on UCB samples. Pathogenic and likely pathogenic mutations were further identified via whole genome sequencing (WGS) and whole exome sequencing (WES). Only donors fulfilling all the above criteria were considered eligible for iPSCs banking.

2.2. GMP-Compliant Operational Procedures. All cell banking procedures were conducted within a Grade B cleanroom environment. Operators followed strict gowning protocols prior to entry, which included hand disinfection, wearing sterile masks (to fully cover the nose and mouth) and hair caps (to enclose all hair), and donning sterile undergarments, coveralls, shoe covers, and gloves, followed by additional hand disinfection using 75% sterile ethanol. All garments were nonshedding and lint-free to minimize particulate release. Operations were performed inside a Class II Type A2 biosafety cabinet (BSC) maintaining a Grade A air quality environment. Sterile instruments, consumables, and equipments were prearranged in the BSC and remained confined within the workspace throughout operations to prevent contamination. The BSC was sanitized by ultraviolet (UV) light irradiation for 1 h prior to each use. After operations, all interior surfaces were thoroughly disinfected with 70% sterile ethanol and subjected to an additional 1 h-UV light treatment to ensure sustained sterility. Environmental monitoring was performed routinely: monthly for settleable microbes and airborne particles in Grade A zone, monthly for settleable microbes, airborne particles and viable microbes in Grade B cleanrooms; and quarterly for settleable microbes and airborne particles in Grade C areas. Cleaning was conducted daily, weekly, and monthly as necessary. Intensive disinfection was performed every 2 weeks using sterile quaternary ammonium compound solution and 75% ethanol alternately. All GMP-compliant materials and reagents used for iPSCs derivation and banking are itemized in Supporting Information 1: Table S4.

2.3. CBMC Isolation and Culture. Frozen UCB units were thawed in a 40°C water bath, transferred to a centrifuge tube, and gently pipetted to ensure uniform distribution. Aliquots for HLA genotyping and STR profiling were aspirated prior to CBMC isolation. The UCB was then diluted 8-fold with sodium chloride injection and centrifuged at $400 \times g$ for 20 min. The pellet was resuspended in sodium chloride

injection to twice the original volume and filtered through a 100 μm strainer. The resulting filtrate was carefully layered over an equal volume of Ficoll-Paque (GE Healthcare) and centrifuged. The middle white layer containing CBMCs was collected and washed twice with sodium chloride injection. The isolated CBMCs were seeded at a density of 1×10^6 cells/mL in a T25 flask. Cells were cultured in StemSpan-ACF Erythroid Expansion Medium supplemented with StemSpan Erythroid Expansion Supplement (Stemcell Technologies) and maintained at 37°C under 5% CO_2 (designated as Day 0). Fresh culture medium was exchanged every other day. The total culture duration did not exceed 18 days, by which time the majority of cells had reached a diameter of 15–17 μm.

2.4. Reprograming of Expanded Erythroid Cells (EECs). On Day 11 of culture, EECs were analyzed by flow cytometry for the expression of CD3, CD19, and CD71. Cells were harvested for reprograming only if they met the following criteria: $CD3^+ < 1\%$, $CD19^+ < 1\%$, and $CD71^+ > 95\%$. EECs were washed twice with StemSpan-ACF Erythroid Expansion Medium. A total of 2×10^6 cells were resuspended in 100 μL of Nucleofector Solution Buffer from the P3 Primary Cell 4D-Nucleofector X Kit L (Lonza), which was premixed with the following reprograming episomal plasmids: pCEP4-OCT4-SOX2, pCEP4-MYC, pCEP4-KLF4, and pCEP4-BCL-XL. Electroporation was carried out using program FI115 on a Lonza 4D Nucleofector system. Following electroporation, cells were allowed to recover for 10 min at 37°C under 5% CO_2 and were then seeded into iMatrix-511-coated 6-well plates. Cells were distributed evenly across one well each in eight independent 6-well plates and cultured in StemSpan-ACF Erythroid Expansion Medium supplemented with StemSpan Erythroid Expansion Supplement at 37°C under 5% CO_2 (designated as Day 0 of reprograming). All wells were sequentially labeled to ensure traceability and prevent handling errors. Sodium butyrate (NaB) was added to the culture medium at a final concentration of 0.25 mM on Day 5. On Day 6, the medium was replaced with CTS Essential 8 Medium (Gibco) supplemented with 0.25 mM NaB. Thereafter, the medium was changed daily using this NaB-supplemented formulation.

2.5. Colony Picking and Selection. All equipment required for colony picking, including a microscope and a tablet computer for documentation, was presterilized and placed inside the BSC. All tools and consumables remained strictly confined within the BSC throughout the procedure to maintain aseptic conditions. Prior to handling, operators disinfected their gloves with 70% sterile ethanol three times. Inside the BSC, colonies exceeding 500 μm in diameter and exhibiting clear physical separation from neighboring colonies were photographed and sequentially numbered to ensure full traceability. Each colony was manually picked using a pipette with sterile 20 μL pipette tip and transferred to individual wells of iMatrix-511-coated 24-well plates (designated as Passage 1). A new tip was used for each colony to prevent cross-contamination; a total of 50 colonies were selected and transferred. Environmental monitoring during the procedure included assessment of settleable microbes and airborne particles inside the BSC. After completion of colony picking, surface microbial testing was conducted on both the work surface within the BSC and the operators' gloves.

2.6. iPSCs Banking and Cryopreservation. Passaging was initiated when colonies at Passage 1 developed dense, phase-bright centers with well-defined edges. Colonies were discarded if they exceeded 8 days in culture at Passage 1, showed significant contamination with nontarget cell types, or displayed poor morphological integrity. Once colonies satisfied these morphological criteria, they were washed with CTS DPBS (1× Gibco) and dissociated with CTS Versene solution (Gibco) for 5 min at 37°C under 5% CO_2. This passaging procedure was used consistently from Passage 1 to Passage 3. Cells from these passages were cultured on iMatrix-511 surfaces in the presence of 10 μM Y27632, which was maintained for 18–24 h postpassaging. Passage 2 cells were grown in 12-well plates and Passage 3 cells in T25 flasks. Throughout all passages, CTS Essential 8 Medium was replaced daily. All qualified colonies were cryopreserved at Passage 3 as cell seed bank (CSB) lines using a cryoprotective medium consisting of 20% CryoSure-DEX40 and 80% CTS Essential 8 Medium supplemented with 10 μM Y27632. Expression of the undifferentiated markers OCT4, SOX2, and NANOG, was analyzed via flow cytometry. Only cell lines exhibiting >70% positivity for these undifferentiated markers were selected for MCB generation. One vial of the optimal CSB line was thawed and recovered into a vitronectin-N-coated T25 flask in CTS Essential 8 Medium and passaged at 60%–80% confluency. Upon reaching Passage 6, cells from 12 T182 flasks were harvested and cryopreserved as the MCB using the same cryoprotective formulation at Passage 3.

2.7. Cell Count and Viability. Cell count and viability were assessed using acridine orange/propidium iodide (AO/PI) staining on a Countstar Rigel S2 instrument. Measurements were taken both before cryopreservation and after thawing one vial of the iPSC MCB lines. All analyses were performed directly in the cryoprotective medium without additional processing.

2.8. Cell and Colony Morphology. Cells were thawed and seeded at a density of $3–4 \times 10^4$ cells/cm^2 into a vitronectin N-coated T25 flask. Cells were initially cultured in CTS Essential 8 Medium supplemented with 10 μM Y27632. After 18–24 h, the medium was exchanged to Y27632-free CTS Essential 8 Medium and replaced daily thereafter. Morphology was monitored and documented on a daily basis.

2.9. HLA (PCR-SBT) and STR (PCR/Capillary Electrophoresis) Analyses. HLA haplotypes (HLA-A, HLA-B, and HLA-DRB1 loci) were confirmed in iPSCs via PCR-based sequencing typing (PCR-SBT). Both HLA haplotypes and STR profiles were cross-verified against the original donor genotypes to confirm cell line identity.

2.10. Analysis of Undifferentiated Markers. Intracellular expression of the transcription factors OCT3/4 and NANOG (undifferentiated markers) was evaluated by flow cytometry. Briefly, 1×10^6 cells were fixed with BD Cytofix Fixation Buffer for 20 min in the dark. After fixation, cells were

washed twice with 1 × Perm/Wash Working Buffer and permeabilized in the same buffer. Aliquots of 5×10^5 cells were stained with BD Pharmingen PerCP-Cy 5.5 Mouse anti-Oct3/4 and BD Pharmingen PE Mouse anti-human Nanog antibodies. Parallel aliquots were stained with corresponding isotype-matched controls. Following PBS washes, fluorescence signals were acquired on a BD FACS Celesta flow cytometer. Surface markers of undifferentiated state (SSEA-4 and TRA-1-60) and the negative marker CD45 were analyzed under nonpermeabilized conditions. For each sample, 5×10^5 cells were stained with BD Pharmingen PE Mouse anti-SSEA-4, BD Pharmingen PE Mouse anti-human TRA-1-60 Antigen, and BD Pharmingen FITC Mouse anti-human CD45 antibodies. Isotype controls were included in separate tubes. Cells were washed with PBS and analyzed using a BD FACS Celesta.

2.11. In Vitro Trilineage Differentiation. MCB cells were thawed and expanded prior to differentiation. A total of 6×10^6 cells were evenly seeded into two wells of an ultra-low attachment 6-well plate and cultured in mTeSR1 medium (Stemcell Technologies) for 18–20 h on a horizontal shaker set at 70 rpm (designated as Day 0). The medium was then replaced with induced differentiation medium under static culture conditions, with medium changes performed every other day for 7 days. Individual embryoid bodies were transferred to Matrigel (Corning)-coated 24-well plates, with 1–2 embryoid bodies per well to facilitate outgrowth. Medium was exchanged every other day until Day 16–Day 18 of differentiation. To validate trilineage differentiation, cells were fixed and subjected to immunofluorescence staining using germ layer-specific markers: alpha-fetoprotein ([AFP] monoclonal antibody [AFP3], Invitrogen) for endoderm, alpha-smooth muscle actin ([α-SMA] monoclonal antibody [1A4], Invitrogen) for mesoderm, and Nestin ([NESTIN] monoclonal antibody [10C2], Invitrogen) for ectoderm. Corresponding IgG isotype controls were included. Parallel samples were analyzed by qPCR for expression of additional germ-layer specific markers. Primer sequences are provided in Supporting Information 2: Table S2.

2.12. In Vivo Trilineage Differentiation. MCB cells were thawed and expanded in culture. A total of 5×10^6 iPSCs were resuspended in a 1:1 mixture of Knockout DMEM/F12 and Matrigel. The cell suspension was subcutaneously injected into the right flank of 6–8-week-old female NCG mice housed under SPF conditions to induce teratoma formation. Teratomas were harvested, fixed in 4% paraformaldehyde, and processed for hematoxylin-eosin (H and E) staining. Histological examination confirmed the presence of tissues representative of all three germ layers, including endoderm-derived glandular structures of the digestive tract, mesoderm-derived cartilage, and ectoderm-derived neural tissue, along with other lineage specific structures.

2.13. Residual Plasmid Detection. MCB cells were thawed and genomic DNA (gDNA) was extracted from 2×10^6 cells. For droplet digital PCR (ddPCR), 100 ng of gDNA was partitioned into droplets via emulsification with droplet generation oil using a QX200 Droplet Generator, in a final reaction volume of 20 μL. Fluorescence signals were detected after PCR amplification using a QX200 Droplet Reader. Parallel qPCR was performed using 100 ng of gDNA with target-specific primers (sequences provided in Supporting Information 3: Tables S2 and S3). The residual plasmid copy number per 100 cells were calculated from ddPCR data using the following formula:

$$\text{Copy number} = \frac{(\text{Sample}^{\text{copies per 20 μL}} - \text{Control}^{\text{copies per 20 μL}}) \times \text{Quantity of extracted gDNA} \times 100}{100\ \text{ng} \times 2 \times 10^6}.$$

Formula 1: Calculation of residual plasmid copy number per 100 cells via ddPCR. Parameters were as follows:

$\text{Sample}^{\text{copies per 20 μL}}$: ddPCR-derived copy number of episomal plasmids (targeting EBNA-1, WPRE, or OriP elements) per 20 μL reaction in iPSCs.

$\text{Control}^{\text{copies per 20 μL}}$: ddPCR-derived copy number of episomal plasmids (targeting EBNA-1, WPRE, or OriP elements) per 20 μL reaction in CBMCs.

Quantity of extracted gDNA: Total mass of gDNA extracted from iPSCs (unit: ng).

100: Normalization factor to report copy number per 100 cells.

2×10^6: Total number of iPSCs used for gDNA extraction.

2.14. Karyotype Analyses. MCB cells were recovered and expanded for karyotype analyses. Chromosomal integrity was assessed through conventional Giemsa staining applied to 100 metaphase cells, alongside G-banding karyotype analysis performed on 50 cells.

2.15. Genomic Analyses. gDNA was extracted from 2×10^6 thawed MCB cells. Both WGS and WES were carried out using next-generation sequencing technologies. WES was conducted with an average coverage depth of 300×. Genomic libraries were prepared with the Hieff NGS OnePot Pro DNA Library Prep Kit V3 (YEASEN) following the manufacturer's instructions. Exome capture was performed using NadPrep Hybrid Capture Reagents (Nanodigmbio Biotechnology Co., Ltd.), followed by high-throughput sequencing on the DNBSEQ-T7 platform (MGI Tech Co., Ltd.) with a variant allele frequency (VAF) detection threshold of 5% (providing 95% sensitivity for mutations present in ≥5% of cells). Raw sequencing data were processed using fastp (v0.22.0) to remove adapter sequences, poly-G tails, and low-quality reads (quality score ≥20 and read length ≥50 bp). High-quality reads were aligned to the GRCh37/hg19 reference

genome using BWA-MEM (v0.7.17) with base quality score recalibration (BQSR). Germline single-nucleotide polymorphisms (SNPs) and insertions/deletions (INDELs) were identified using HaplotypeCaller (GATK v4.2.6), and somatic variants were detected with MuTect2. Copy number variations (CNVs) were called using CNVkit (v0.9.6). All detected variants were functionally annotated with ANNOVAR (hg19_refGene). For WGS, an average depth of 45× was achieved. Library preparation was conducted using the same Hieff NGS OnePot Pro DNA Library Prep Kit V3, and sequencing was performed on the DNBSEQ-T7 platform (MGI Tech Co., Ltd.) under identical sensitivity criteria (5% VAF threshold, 95% sensitivity for ≥5% cellular prevalence). Data processing, read alignment, and germline variant calling were consistent with the WES workflow. Additionally, structural variants (SVs) were detected using Manta (v1.6.0). Functional annotation of all variants was performed using ANNOVAR as described above.

2.16. Sterility Testing. Eight vials of iPSC MCB were thawed and seeded into a vitronectin N-coated T182 flask at a density of 4×10^4 cells/cm^2 in CTS Essential 8 Medium supplemented with 10 μMY27632. After 18–24 h, the medium was replaced with Y27632-free CTS Essential 8 medium. Cells were maintained under these conditions for 72 h without further treatment. The cell culture supernatant was then collected, centrifuged, and the clarified supernatant was subjected to sterility and mycoplasma testing. Sterility was assessed using the membrane-filtration method in compliance with the Pharmacopeia of the People's Republic of China.

2.17. Mycoplasma Testing. Mycoplasma detection was conducted on the same clarified supernatant sample described in Section 2.16 using qPCR with a MycoSEQ kit (Thermo Fisher Scientific).

2.18. Endotoxin Testing. Endotoxin levels were measured using a Toxinometer ET-6000 (FUJIFILM Wako Pure Chemical Corporation) in accordance with the manufacturer's instructions.

2.19. Virus Testing. Viral safety testing was performed on both the original UCB units and the final iPSC MCB. Enzyme-linked immunosorbent assay (ELISA) was used to screen UCB for human T-lymphotropic leukemia virus (HTLV), Epstein-barr virus (EBV), human parvovirus B19 (B19V), and herpes simplex virus type 1 (HSV-I) and herpes simplex virus 2 (HSV-II). The iPSC MCB was tested via ELISA for an extended panel of human viruses, including EBV, human cytomegalovirus (HCMV), human retroviruses (HIV-1/2 and HTLV-1/2), human hepatitis viruses (HAV, HBV, and HCV), B19V, human papillomavirus (HPV), human polyomavirus (BKV), human adenovirus (ADV), and human herpes viruses 6/7/8 (HHV-6/7/8).

3. Results

3.1. Donor Selection and Quality Control. HLA-homozygous frozen UCB samples with informed consent forms were obtained from the Tianjin Cord Blood Public Bank and rigorously screened. A donor exhibiting the HLA-genotype HLA-A*30:01,30:01, HLA-B*13:02, 13:02, HLA-C*06:02, 06:02, HLA-DRB1*07:01, 07:01, and HLA-DQB1*02:02 haplotype, the most frequent five-locus homozygous HLA genotype in the Chinese population, was selected. All donor consent documentation and quality control evaluations were completed prior to UCB banking. To identify the optimal UCB sample, four strict quality control criteria were enforced: male donors with blood type O were prioritized to minimize risks related to X chromosome inactivation [22]; sterility and viral-free status were confirmed through plasma testing for HTLV, EBV, B19V, HSV-I and HSV-II, with all results negative; STR analysis across 21 allelic markers verified donor identity and exclude maternal blood contamination; and WGS as well as WES analyses were performed to screen for pathogenic and likely pathogenic mutations, thereby reducing hereditary risk. HLA haplotype analysis based on WES data confirmed homozygosity, consistent with documented records. These stringent and comprehensive screening measures significantly minimized potential risks in large-scale iPSCs banking.

3.2. Production of GMP-Compliant hiPSCs. Frozen UCB meeting the above criteria was thawed, and CBMCs were isolated via Ficoll density gradient centrifugation. CBMCs were cultured to expand and induce erythroid differentiation of human hematopoietic progenitor cells. When large, presumptive erythroblast-like cells constituted the dominant population, these EECs underwent intermediate process release testing. EECs displaying $CD3^+ < 1\%$, $CD19^+ < 1\%$ and $CD71^+ > 95\%$, a profile associated with high reprograming efficiency, were released for subsequent procedures. The hiPSCs were generated by electroporation of EECs with episomal plasmids (pCEP4-OCT4-SOX2, pCEP4-MYC, pCEP4-KLF4, and pCEP4-BCL-XL) [25, 26]. A total of 2×10^6 cells were evenly seeded into eight wells of 6-well plates. Notably, increased seeding wells were correlated with more efficient generation of single colonies to a certain extent. Furthermore, reprograming efficiency was higher when using iMatrix-511 as substrate compared to Vitronectin-N (data not shown).

Primary iPSC colonies (Passage 0) were cultured in CTS Essential 8 Medium supplemented with NaB under hypoxia conditions (3% O_2). Postelectroporation, the addition of the CEPT cocktail significantly enhanced reprograming efficiency and shortened the colony formation time [27]. A total of 50 independent single colonies were selected based on the following morphology criteria: tightly clustered growth, uniform dome-shaped morphology with defined edges, compact cell–cell contact, high nucleus-to-cytoplasm ratio, and absence of nontarget cells. These colonies were manually picked under a microscope and individually transferred to separate wells of 24-well plates as Passage 1 cultures. Subsequent expansion was carried out with strict selection criteria: among the 50 initial colonies, 41 successfully expanded and were passaged within 8 days; the remaining nine were discarded due to poor survival or limited proliferation capacity. By Passage 3, 34 colonies remained, with seven discarded (six due to excessive nontarget cells and one due to poor quality). All 34 colonies at Passage 3

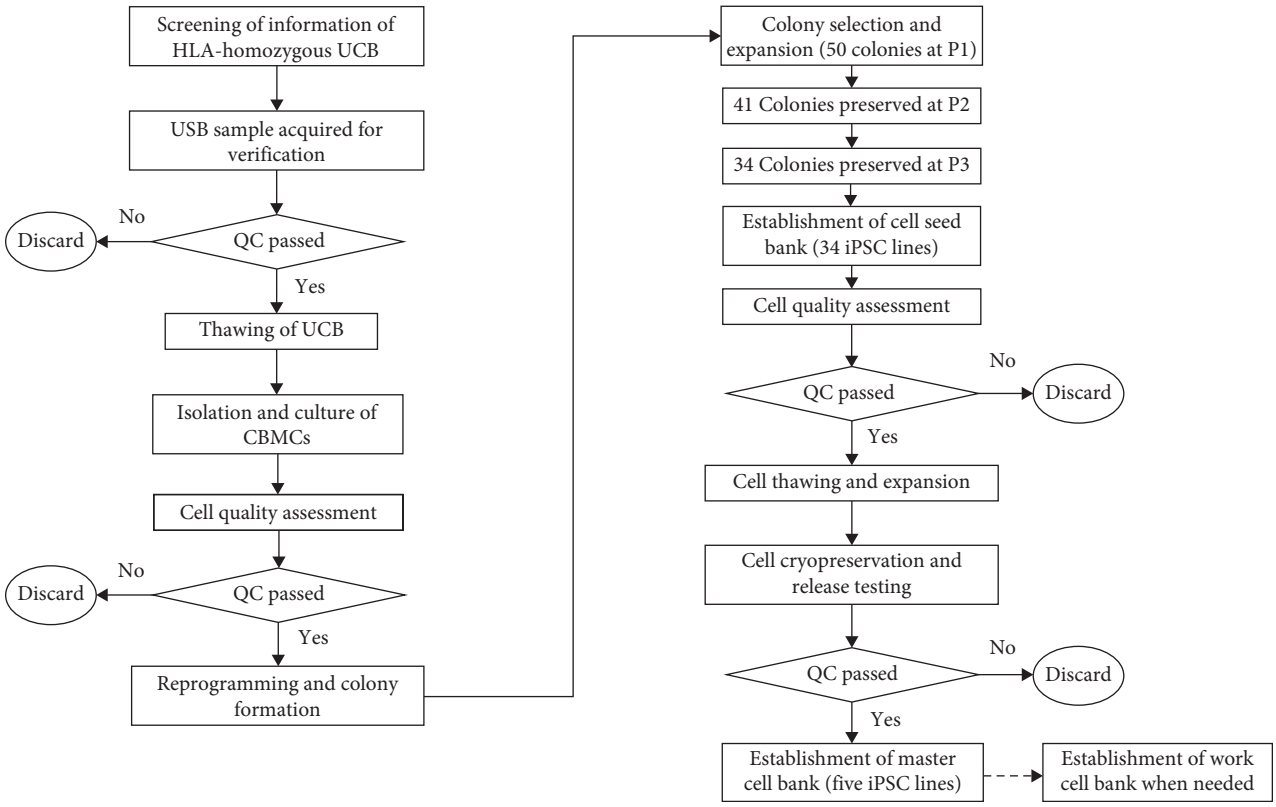

FIGURE 1: Workflow for the establishment of a GMP-compliant hiPSC banking. hiPSC lines were generated from UCB and systematically expanded through sequential banking stages: CSB, MCB, and WCB. Critical quality control checkpoints are integrated throughout the process to ensure product safety and compliance.

were cryopreserved as CSB lines. Five CSB lines were sequentially expanded and cryopreserved as MCB lines (Passage 6). The remaining CSB lines remain available for future GMP-compliant expansion and MCB establishment following successful release testing. Notably, five distinct single-colony-derived iPSC MCB lines were established in a sequential manner to prevent cross-contamination. Prior to cryopreservation, cell confluency was strictly maintained between 60% and 80%. Each MCB line consisted of 100–200 cryovials, with 1.5×10^6 cells per vial. This confluency threshold was implemented based on observations that two of the five iPSC MCB lines exhibited poor post-thaw survival and seeding efficiency, which was primarily attributed to high confluency (>90%) at the time of cryopreservation. After passing all hiPSC-specific quality control release tests (described in subsequent sections), one vial of an MCB line was thawed and expanded to Passage 9 to establish working cell bank (WCB) as needed (Figure 1). To ensure full GMP compliance throughout hiPSC generation, all raw materials adhered to GMP standards, all manufacturing steps were conducted in a GMP-compliant facility, all procedures followed approved standard operating procedures (SOPs), and all operations were thoroughly documented.

3.3. QC Tests and Product Release. The establishment of standardized acceptance criteria for the release of MCB and WCB products remains challenging, largely due to the difficulties in validating detection assay methodologies [28]. To address this, we propose a set of recommended quality control test parameters and corresponding release criteria for iPSC MCB lines, as summarized in Table 1.

To define the quality standards for the qualification of iPSC MCB under GMP-compliant conditions, the following criteria were applied: postcryopreservation cell viability must exceed 70%, with iPSC colonies exhibiting well-defined borders, tight cell–cell contact, and a high nucleus-to-cytoplasm ratio [22]. Surface markers of undifferentiated state (SSEA4 and TRA-1-60) must show positivity in ≥90% of cells, while nuclear markers (OCT3/4 and NANOG) require ≥90% and ≥70% positive expression, respectively. The negative marker CD45 should be detectable in ≤2% of cells. Additionally, markers representative of all three germ layers (endoderm, mesoderm, and ectoderm) should be detectable following both in vitro differentiation [29] and in vivo spontaneous teratoma formation [30]. Cells fulfilling these release criteria demonstrated high quality in terms of pluripotency and functional utility. For cell therapy safety, residual episomal plasmids were rigorously assessed by analyzing at least two targets, each with a threshold of ≤1 plasmid copy per 100 cells [31]. Should this value be exceeded, cells undergo five additional passages followed by retesting; lines with persistently elevated plasmid copy number are deemed unsuitable for use. Chromosomal integrity was evaluated by examining a minimum of 100 metaphases for numerical, morphological, and structural abnormalities, with at least 50 metaphases analyzed by micrography and karyotyping. WGS and

Table 1: Quality control and release criteria for iPSC master cell bank.

Category	Test name	Test method	Acceptance criteria
Cell activity	Cell viability	AO/PI staining	>70% Viability postcryopreservation
	Living cell number	AO/PI staining	$\geq 1 \times 10^6$ Cells/vial
Cell line identity	Cellular morphology	Microscopic examination	Colony growth with smooth edge and cells in tight contact with each other
	HLA haplotype	SBT	Identical to starting material
	STR profiling	SBT	Identical to starting material
	Undifferentiated markers	Flow cytometry	≥90% Positive for SSEA4, TRA-1-60 and OCT3/4, ≥70% for NANOG, ≤2% for CD45
Potency	Trilineage differentiation in vitro	Embryoid body induction	Positive for each germ layer
	Trilineage differentiation in vivo	Teratoma formation	Positive for each germ layer
Purity/impurity	Residual plasmid	ddPCR	≤1 Plasmid copy per 100 cells; or reduction after 5 additional passages
Genetic stability	Karyotyping	G-banding	Normal (diploid) in 50 metaphases
	Whole-genome sequencing	NGS	No pathogenic or likely pathogenic mutations in tumor-associated and genetic correlation genes
	Whole-exome sequencing	NGS	No pathogenic or likely pathogenic mutations in tumor-associated and genetic correlation genes
Safety	Sterility	Membrane filtration	Negative
	Mycoplasma	Culture-based method	Negative
	Endotoxin	Gel method	<5.0 EU/mL
	Adventitious human viruses	ELISA	Negative

WES analyses must confirm the absence of pathogenic and likely pathogenic mutations. All tested MCB lines should show negative results in sterility testing (via membrane filtration), mycoplasma detection (culture-based methods), endotoxin assays (gel method, <5.0 EU/mL), and adventitious human viruses testing (ELISA for EBV, HCMV, HIV-1/2, HTLV-1/2, HAV, HBV, HCV, B19V, HPV, BKV, ADV, and HHV-6/7/8). Taken together, these criteria established comprehensive quality standards for iPSC MCB manufactured under GMP-compliant conditions.

3.4. Characterization of iPSCs

3.4.1. Pluripotency and Differentiation. The iPSC MCB lines exhibited typical embryonic stem cell (ESC)-like morphology, forming colonies with well-defined edges and tight cell–cell contact (Figure 2A). The majority of iPSCs tested positive for alkaline phosphatase (AP) activity (Figure 2B). qPCR analysis demonstrated that mRNA expression levels of the undifferentiated markers OCT4, SOX2, and NANOG were comparable to those in ESCs and significantly higher than in EECs (Figure 2C). Flow cytometry and immunofluorescence staining confirmed strong expression of both surface and nuclear undifferentiated markers (Figure 2D, E). Furthermore, the iPSCs successfully differentiated into derivatives of all three germ layers, as confirmed through in vitro embryoid body formation and in vivo teratoma assays (Figure 2F, H). Taken together, these results confirmed that the GMP-compliant iPSCs maintain high pluripotency and multilineage differentiation potential.

3.4.2. Genomic Stability. For safety evaluation, residual episomal plasmid copy numbers were quantified in three iPSC MCB lines via ddPCR. All lines showed fewer than one episomal plasmid copy number per 100 cells (Figure 3A). No amplification was detected within 35 cycles by qPCR (Supporting Information 4: Table S1), resulting in a 100% pass rate for episomal plasmid residual testing in the evaluated iPSC MCB lines. Since all three iPSC MCB lines met the clearance criteria, further passaging and retesting were not required. Karyotype analysis revealed no structural or numerical chromosomal abnormalities in any of the three iPSC MCB lines (Figure 3B). To assess tumorigenic and germline variations, iPSC MCB lines were compared with original UCB cells using the ACMG genetic variation classification criteria and ClinGen guidelines. The analysis covered gene-disease associations, variant pathogenicity, variant carrying status, and inheritance patterns. Results indicated that none of the three iPSC MCB lines carried known pathogenic genetic variations. No loss-of-function mutations, such as point mutations, small fragment INDELs, or large fragment CNVs, were detected. Moreover, no de novo mutations were introduced during iPSCs generation or expansion. HLA haplotype and STR profiles remained identical to those of the starting material (Supporting Information 2: Figure S1).

3.4.3. Safety Testing. Sterility and mycoplasma tests yielded negative results. Pathogen-specific testing confirmed negativity for EBV, HCMV, HIV-1/2, HTLV-1/2, HAV, HBV, HCV, B19V, HPV, BKV, ADV, and HHV-6/7/8. Endotoxin levels

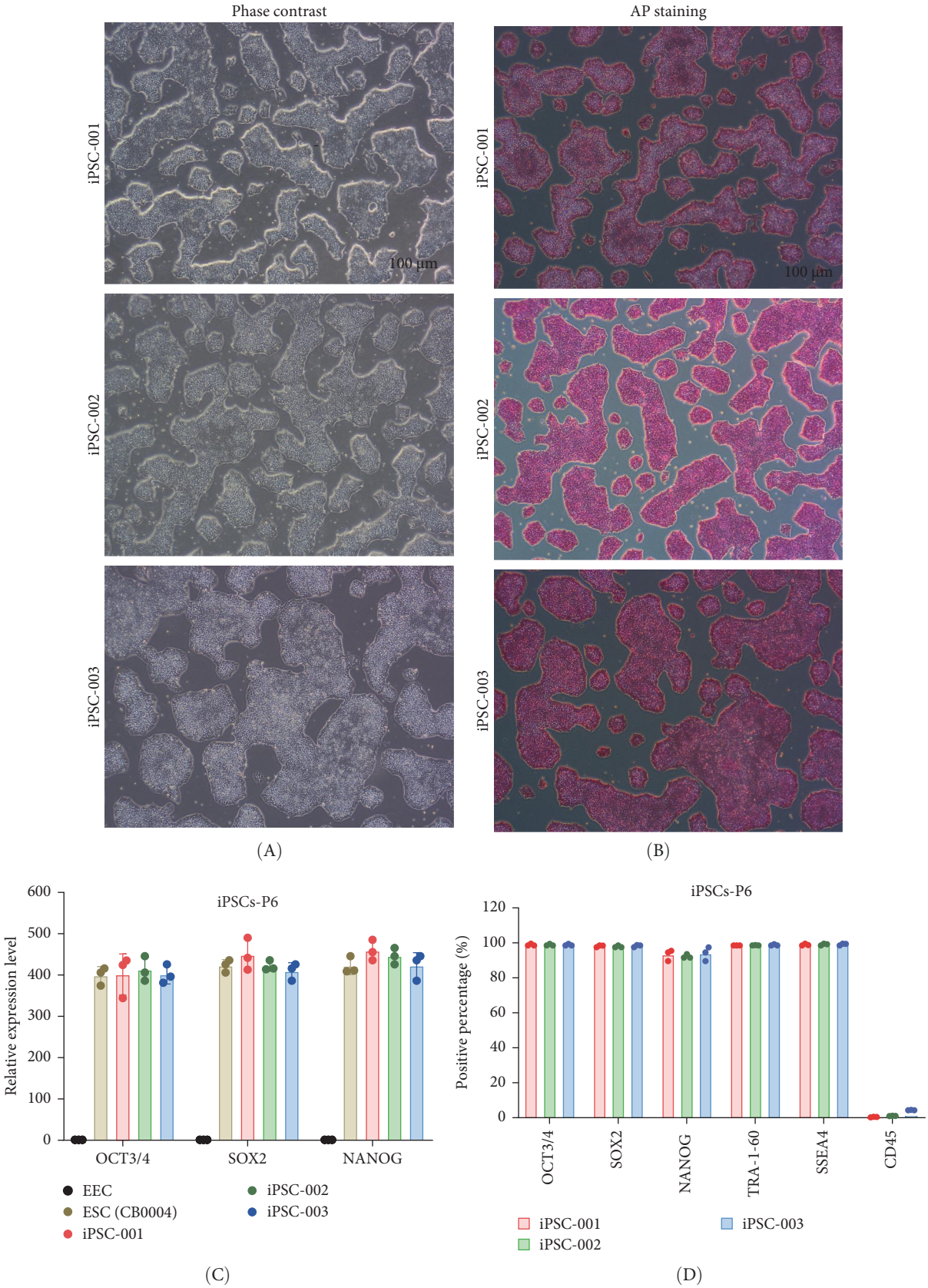

Figure 2: Continued.

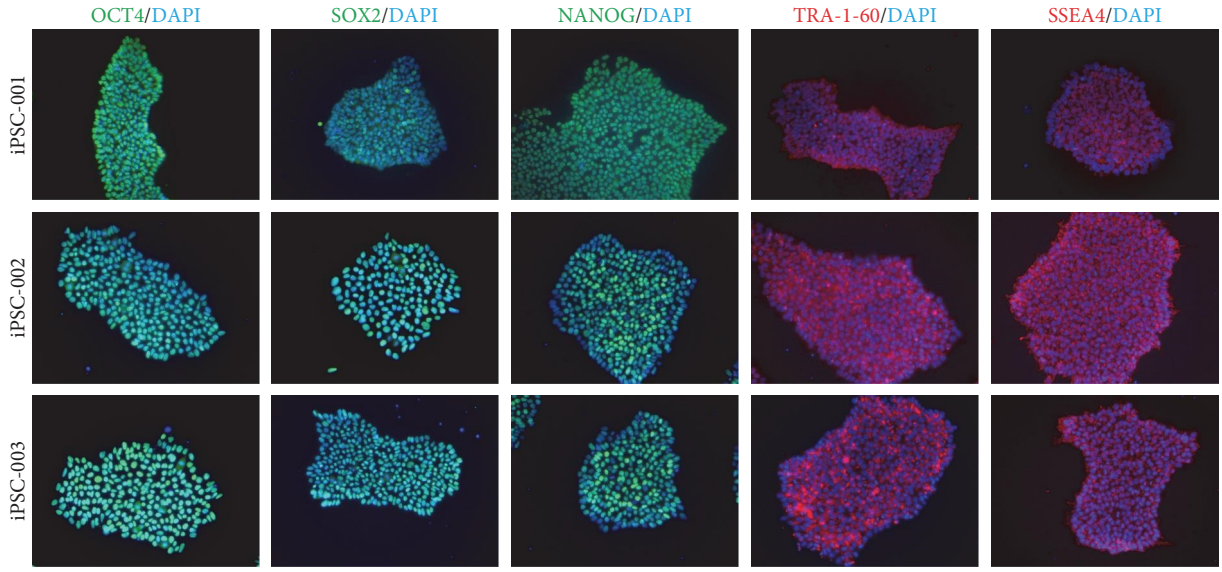

(E)

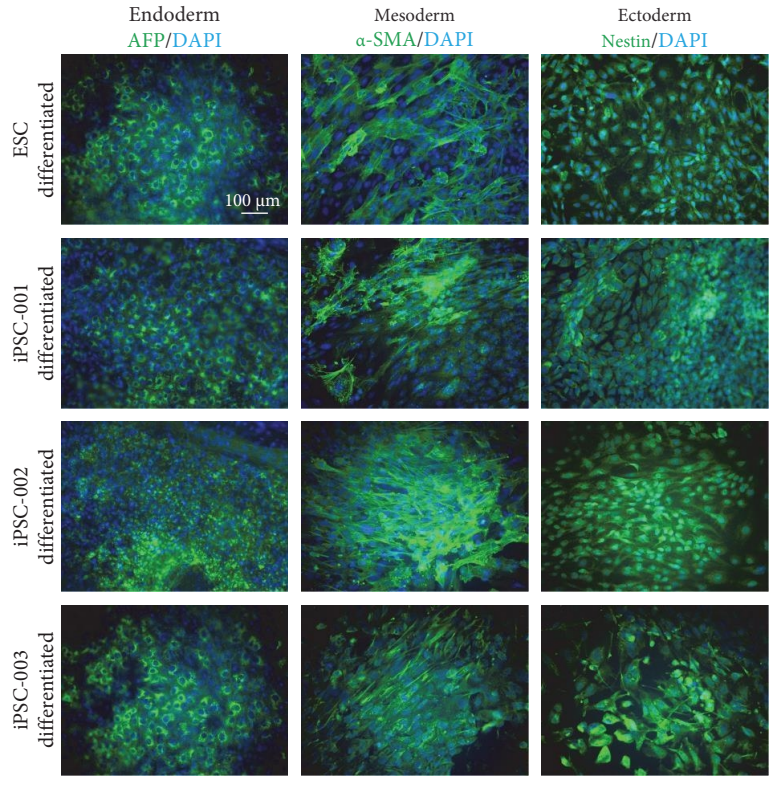

(F)

Figure 2: Continued.

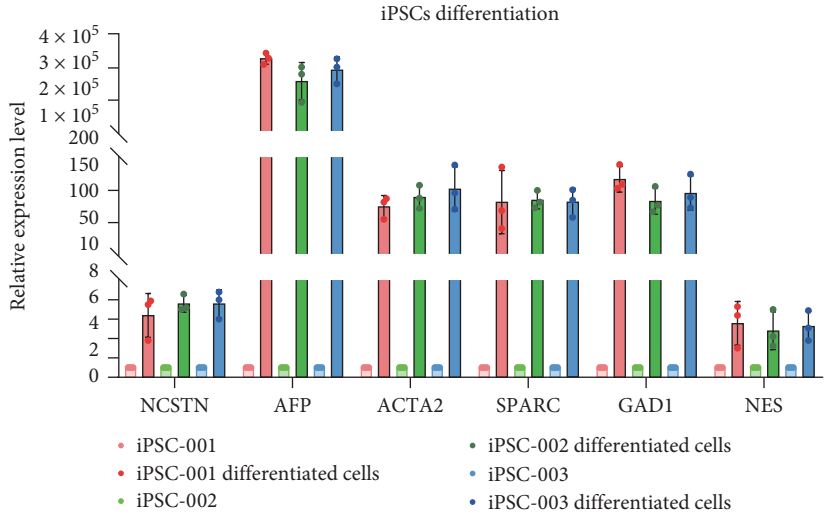

(G)

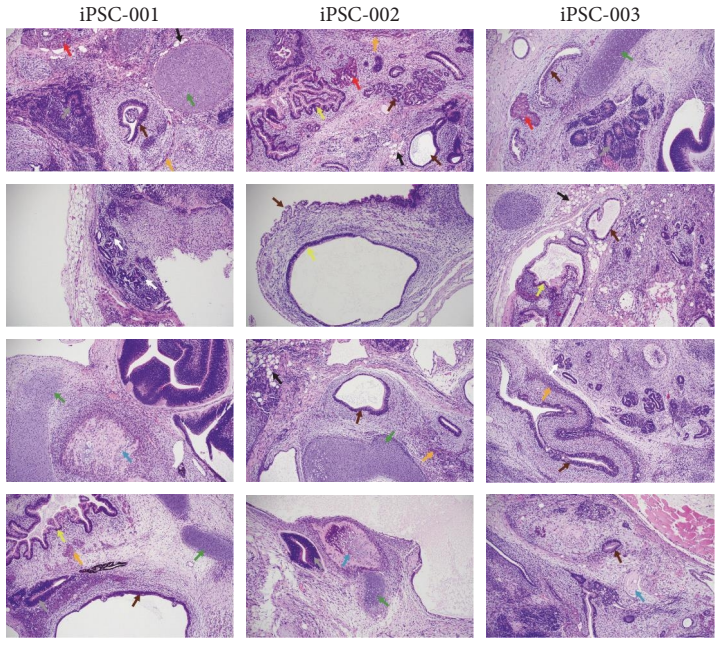

(H)

Figure 2: Pluripotency characterization of iPSC MCB lines. (A, B) Representative phase-contrast images showed the typical morphology of the three iPSC MCB lines before (A) and after AP staining (B). Scale bar: 100 μm. (C–E) Expression of undifferentiated markers was evaluated by qPCR for relative mRNA expression levels to EECs (C), flow cytometry (D), and immunofluorescence staining (E) for protein expression. Data shown are mean ± SEM from three biological replicates. Scale bar: 100 μm. (F, G) Trilineage differentiation potential was assessed via embryoid body formation. Immunofluorescence staining (F) and qPCR (G) were used to evaluate endoderm, mesoderm, and ectoderm marker expression. Data shown are mean ± SEM from three biological replicates. Scale bar: 100 μm. (H) Expanded iPSC MCB lines were and injected into NGG mice, leading to spontaneously teratoma formation. Tumors were excised and subjected to H and E staining. Representative images show iPSCs differentiation into tissues of the three germ layers, identified by characteristic morphological features. Endoderm-derived tissues include hepatic tissue (red arrow, characterized by isolated clusters of hepatocytes with eosinophilic cytoplasm and visible sinusoid-like spaces), as well as mucosal epithelium of the digestive/respiratory tract (yellow arrow, identified by the presence of single-layered columnar epithelial cells containing goblet cells and accompanying lumen formation). Mesoderm-derived tissues are observed as bone tissue (blue arrow, featured by mineralized matrix with osteocyte lacunae), cartilage tissue (green arrow, recognized by chondrocytes in lacunae within a basophilic extracellular matrix), muscle tissue (orange arrow, characterized by elongated, striated eosinophilic muscle fibers), adipose tissue (black arrow, marked by large intracellular vacuoles compressing the nucleus toward the periphery), and renal tissue (white arrow, distinguished by primitive glomerular-like capillary loops and early tubular structures). Ectoderm-derived neural tissue (gray arrow) is marked by rosette-like structures formed by primitive neuroblasts surrounding eosinophilic neuropil; the nuclei are peripherally located with cytoplasm converging centrally. Partially undifferentiated glandular structures (brown arrow) consist of disorganized epithelial tubules lacking mature tissue-specific architecture.

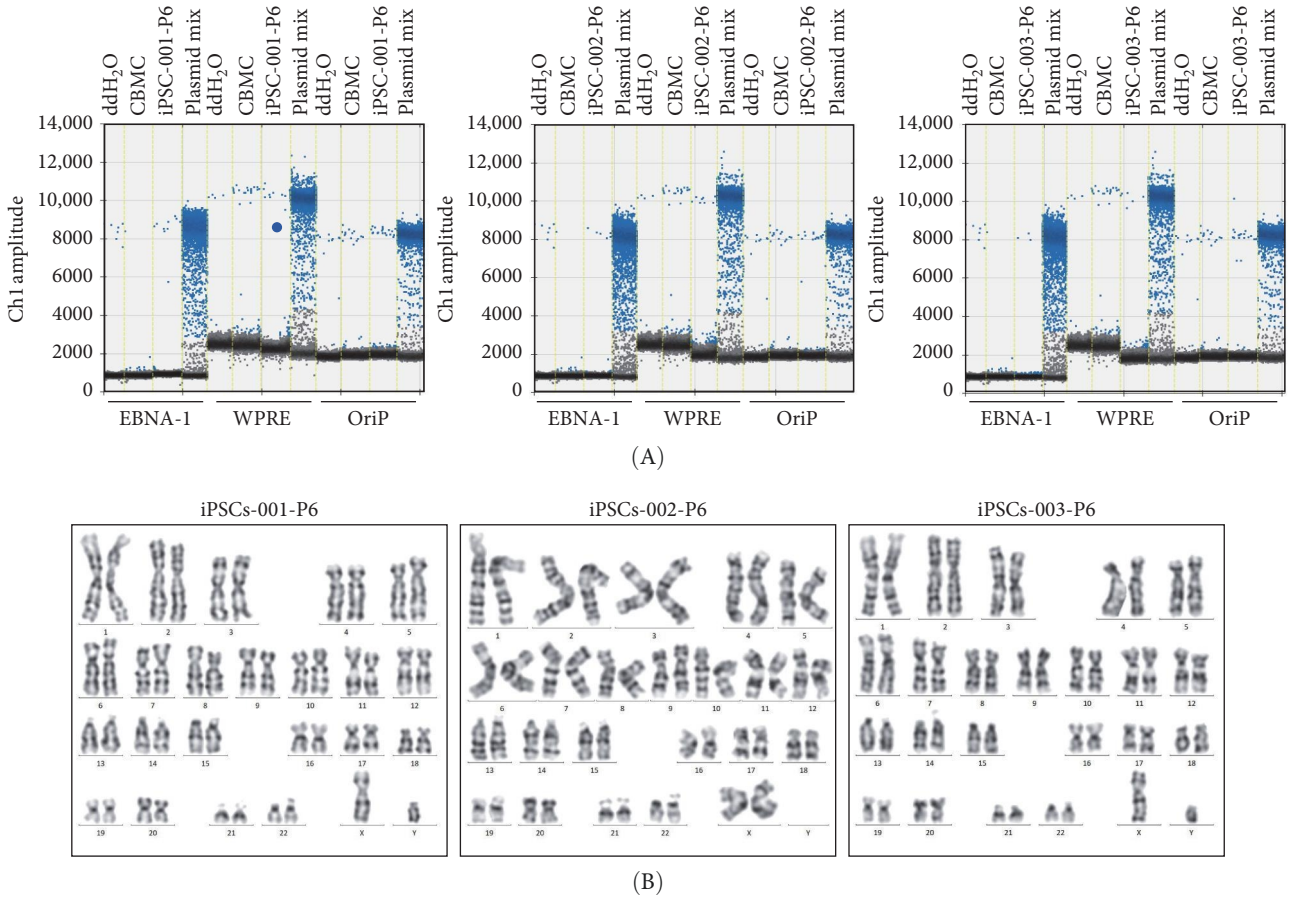

FIGURE 3: Safety analysis of iPSC MCB lines. (A) Residual episomal plasmids were quantified in iPSC MCB lines using ddPCR with probes targeting EBNA-1, WPRE, and OriP. (B) Representative G-banding karyotype images demonstrated normal chromosomal structure and number in iPSC MCB lines.

were measured below 5.0 EU/mL, complying with the predefined acceptance criterion.

In summary, all iPSC lines produced under GMP-compliant conditions satisfied the established release criteria, supporting their suitability for subsequent multidirectional differentiation and potential use in clinical cell therapy applications.

4. Discussion

Mononuclear cells isolated from UCB represent a highly suitable starting material for iPSCs generation due to their capacity for efficient reprograming following a brief and straightforward culture period. For human hematopoietic progenitor cells derived from UCB, expansion and erythroid differentiation typically require approximately 8 days when using fresh samples and 12 days for frozen UCB. Moreover, EECs exhibit greater homogeneity compared with isolated CBMCs, supporting significantly improved reprograming efficiency [19]. Reprograming efficiency can be further enhanced by supplementing the transfection with episomal plasmids carrying factors such as BCL-XL and EBNA1 [17, 25, 26]. Importantly, the addition of the CEPT cocktail [27] postelectroporation resulted in a 5.66-fold increase in reprograming efficiency and reduced the time required for monoclonal formation to 1 week (data not shown).

In assessing the quality of hiPSCs, we performed a comprehensive evaluation that included the parameters summarized in Table 1, covering cell cycle profiling, population doubling time, and pluripotency verification via immunofluorescence staining, AP staining, and qPCR. Nevertheless, quality control and release criteria remain inconsistently applied across research institutions. The establishment of standardized acceptance parameters for MCB and WCB quality presents a challenge, largely owing to the complexity of validating detection methods. Therefore, the development of stable and reliable analytical methods is essential for defining universally applicable release criteria.

Notably, two iPSC MCB lines produced under GMP-compliant conditions exhibited suboptimal post-thaw survival rates, despite meeting all predefined release criteria for cell viability and total viable cell count. Further investigation identified the physiological state at the time of cryopreservation as a critical determinant influencing post-thaw survival. Parameters

including culture medium volume, feeding frequency, and cell confluency prior to cryopreservation must be carefully monitored and controlled to ensure consistent cell quality and functionality after recovery.

5. Conclusions

In this study, we successfully established GMP-compliant HLA-homozygous iPSC lines derived from UCB and developed a comprehensive set of quality control standards for their characterization. All iPSC MCB lines not only satisfied our stringent release criteria but also exhibited high pluripotency and robust capacity for multidirectional differentiation, confirming their suitability for use in advanced iPSC-based cell therapies. The GMP-compliant iPSCs banking platform presented here offers a standardized, reproducible, and cost-effective framework for iPSCs banking, with the potential to provide a reliable source of high-quality iPSC lines for future clinical applications.

Data Availability Statement

The data that support the findings of this study are available on request from the corresponding author.

Ethics Statement

Human cryopreserved UCB units were obtained from the Tianjin Cord Blood Public Bank. All donors were thoroughly informed of the study's purpose and procedures, and provided written informed consent forms prior to UCB donation. The study was conducted in accordance with the ethical principles of the Declaration of Helsinki and was approved by the Ethics Committee of the Institute of Hematology and Blood Diseases Hospital (Approval Number: YW2018001-EC-1). All animal experiments were performed under a protocol reviewed and approved by the Experimental Animal Ethics Committee of Youji (Tianjin) Pharmaceutical Technology Co., Ltd.

Conflicts of Interest

The authors declare no conflicts of interest.

Author Contributions

The study was conceptualized by Yu Zhang and Wei Du. The manuscript was drafted by Qianping Zhang and revised by Qianping Zhang and Xiaohui Shi. The experiments were guided by Qianping Zhang and conducted by Lijuan Cui, Ying Jia, Xiaohui Shi and Jinmei Zhang. Technical and experimental support were provided by Li Zhang, Zhihui Liu, Yun Zhang, Huizhuan Fu, Qi Qi and Quan Chen.

Funding

This work was supported by the Tianjin Science and Technology Plan Innovation Platform Special Support Program (Grant 18PTSYJC00070), the Tianjin Postdoctoral Support Program (Grant TJQYBSH2018030), the National Key Research and Development Program of China (Grant 2025YFC3410100), the Science and Technology Project of Wuhan (Grant 2025020602030091), the Haihe Laboratory of Cell Ecosystem Innovation Fund (Grant HH22KYZX0046), and the Tianjin Free Trade Zone Innovation Development Project 211 (Grant ZMCY-03–2021002-01).

Acknowledgments

The authors sincerely acknowledge Tianjin Cord Blood Bank for the provision of cord blood resources and dedicated technical guidance.

Supporting Information

Additional supporting information can be found online in the Supporting Information section.

Supporting Information 1. Detection of episomal plasmid residuals for three targets (EBNA1, WPRE, and OriP). The no-template control (NTC) and EECs were used as negative controls, and the plasmid was used as a positive control. The Supporting Table S1 presents the plasmid residual results for three iPSC lines.

Supporting Information 2. STR profiling of established iPSCs. In this test report, the serial number BP245867OO refers to the donor cord blood sample, BP245868OO to iPSC-001, BP245869OO to iPSC-002, and BP245870OO to iPSC-003. Peak diagrams of 21 allele markers are shown in sequence.

Supporting Information 3. Primers used in qPCR analyses for detecting targets on the episomal plasmids and markers of the three germ layers are presented in Supporting Tables S2 and S3 respectively.

Supporting Information 4. GMP compliance of critical reagents for iPSC banking are listed in Supporting Table S4.

References

[1] K. Takahashi and S. Yamanaka, "Induction of Pluripotent Stem Cells From Mouse Embryonic and Adult Fibroblast Cultures by Defined Factors," *Cell* 126, no. 4 (2006): 663–676.

[2] K. Takahashi, K. Tanabe, M. Ohnuki, et al., "Induction of Pluripotent Stem Cells From Adult Human Fibroblasts by Defined Factors," *Cell* 131, no. 5 (2007): 861–872.

[3] J. Yu, M. A. Vodyanik, K. Smuga-Otto, et al., "Induced Pluripotent Stem Cell Lines Derived From Human Somatic Cells," *Science* 318, no. 5858 (2007): 1917–1920.

[4] H. Okano, D. Yasuda, K. Fujimori, S. Morimoto, and S. Takahashi, "Ropinirole, a New ALS Drug Candidate Developed Using iPSCs," *Trends in Pharmacological Sciences* 41, no. 2 (2020): 99–109.

[5] S. Yamanaka, "Pluripotent Stem Cell-Based Cell Therapy—Promise and Challenges," *Cell Stem Cell* 27, no. 4 (2020): 523–531.

[6] S. Wang, Y. Du, B. Zhang, et al., "Transplantation of Chemically Induced Pluripotent Stem-Cell-Derived Islets Under Abdominal Anterior Rectus Sheath in a Type 1 Diabetes Patient," *Cell* 187, no. 22 (2024): 6152–6164.e18.

[7] T. Soma, Y. Oie, H. Takayanagi, et al., "Induced Pluripotent Stem-Cell-Derived Corneal Epithelium for Transplant Surgery: A Single-Arm, Open-Label, First-in-Human Interventional Study in Japan," *The Lancet* 404, no. 10466 (2024): 1929–1939.

[8] M. Mandai, A. Watanabe, Y. Kurimoto, et al., "Autologous Induced Stem-Cell–Derived Retinal Cells for Macular Degeneration," *New England Journal of Medicine* 376, no. 11 (2017): 1038–1046.
[9] F. T. Merkle, S. Ghosh, N. Kamitaki, et al., "Human Pluripotent Stem Cells Recurrently Acquire and Expand Dominant Negative P53 Mutations," *Nature* 545, no. 7653 (2017): 229–233.
[10] H. Zhou, H. Martinez, B. Sun, et al., "Rapid and Efficient Generation of Transgene-Free IPSC From a Small Volume of Cryopreserved Blood," *Stem Cell Reviews and Reports* 11, no. 4 (2015): 652–665.
[11] Y. Xi, G. Yue, S. Gao, R. Ju, and Y. Wang, "Human Umbilical Cord Blood Mononuclear Cells Transplantation for Perinatal Brain Injury," *Stem Cell Research & Therapy* 13, no. 1 (2022): 458.
[12] X. Meng, A. Neises, R.-J. Su, et al., "Efficient Reprogramming of Human Cord Blood CD34+ Cells Into Induced Pluripotent Stem Cells With OCT4 and SOX2 Alone," *Molecular Therapy* 20, no. 2 (2012): 408–416.
[13] K. M. Abberton, T. L. McDonald, M. Diviney, et al., "Identification and Re-Consent of Existing Cord Blood Donors for Creation of Induced Pluripotent Stem Cell Lines for Potential Clinical Applications," *Stem Cells Translational Medicine* 11, no. 10 (2022): 1052–1060.
[14] K. Okita, T. Yamakawa, Y. Matsumura, et al., "An Efficient Nonviral Method to Generate Integration-Free Human-Induced Pluripotent Stem Cells From Cord Blood and Peripheral Blood Cells," *Stem Cells* 31, no. 3 (2013): 458–466.
[15] M. Turner, S. Leslie, N. G. Martin, et al., "Toward the Development of a Global Induced Pluripotent Stem Cell Library," *Cell Stem Cell* 13, no. 4 (2013): 382–384.
[16] S. Sugita, Y. Iwasaki, K. Makabe, et al., "Lack of T Cell Response to IPSC-Derived Retinal Pigment Epithelial Cells From HLA Homozygous Donors," *Stem Cell Reports* 7, no. 4 (2016): 619–634.
[17] S. Yoshida, T. M. Kato, Y. Sato, et al., "A Clinical-Grade HLA Haplobank of Human Induced Pluripotent Stem Cells Matching Approximately 40% of the Japanese Population," *Med* 4, no. 1 (2023): 51–66.e10.
[18] S. Lee, J. Y. Huh, D. M. Turner, et al., "Repurposing the Cord Blood Bank for Haplobanking of HLA-Homozygous IPSCs and Their Usefulness to Multiple Populations," *Stem Cells* 36, no. 10 (2018): 1552–1566.
[19] P. Tian, A. Elefanty, E. G. Stanley, J. C. Durnall, L. H. Thompson, and N. J. Elwood, "Creation of GMP-Compliant IPSCs From Banked Umbilical Cord Blood," *Frontiers in Cell and Developmental Biology* 10 (2022).
[20] J. J. Novoa, I. M. Westra, E. Steeneveld, et al., "Good Manufacturing Practice–Compliant Human Induced Pluripotent Stem Cells: From Bench to Putative Clinical Products," *Cytotherapy* 26, no. 6 (2024): 556–566.
[21] B. Kuebler, B. Alvarez-Palomo, B. Aran, et al., "Generation of a Bank of Clinical-Grade, HLA-Homozygous iPSC Lines With High Coverage of the Spanish Population," *Stem Cell Research & Therapy* 14, no. 1 (2023): 366.
[22] M. Alowaysi, R. Lehmann, M. Al-Shehri, et al., "HLA-Based Banking of Induced Pluripotent Stem Cells in Saudi Arabia," *Stem Cell Research & Therapy* 14, no. 1 (2023): 374.
[23] L. R. Beckenkamp, C. G. da Silva, M. L. I. Von Hohendorff, and K. S. Ogliari, "Manufacturing Parameters for the Creation of Clinical-Grade Human-Induced Pluripotent Stem Cell Lines From Umbilical Cord Mesenchymal Stromal Cells," *Stem Cells Translational Medicine* 13, no. 5 (2024): 454–461.
[24] X. Zhu, B. Tang, and Z. Sun, "Umbilical Cord Blood Transplantation: Still Growing and Improving," *Stem Cells Translational Medicine* 10, no. S2 (2021): S62–S74.
[25] Z. Ivanovic, R.-J. Su, D. J. Baylink, et al., "Efficient Generation of Integration-Free iPS Cells From Human Adult Peripheral Blood Using BCL-XL Together With Yamanaka Factors," *PLoS ONE* 8, no. 5 (2013): e64496.
[26] B.-K. Chou, H. Gu, Y. Gao, et al., "A Facile Method to Establish Human Induced Pluripotent Stem Cells From Adult Blood Cells Under Feeder-Free and Xeno-Free Culture Conditions: A Clinically Compliant Approach," *Stem Cells Translational Medicine* 4, no. 4 (2015): 320–332.
[27] Y. Chen, C. A. Tristan, L. Chen, et al., "A Versatile Polypharmacology Platform Promotes Cytoprotection and Viability of Human Pluripotent and Differentiated Cells," *Nature Methods* 18, no. 5 (2021): 528–541.
[28] J. Novoa, I. Westra, E. Steeneveld, et al., "Validating Human Induced Pluripotent Stem Cell-Specific Quality Control Tests for the Release of an Intermediate Drug Product in a Good Manufacturing Practice Quality System," *Cytotherapy* 26, no. 9 (2024): 1105–1117.
[29] S. Rungarunlert, "Embryoid Body Formation From Embryonic and Induced Pluripotent Stem Cells: Benefits of Bioreactors," *World Journal of Stem Cells* 1, no. 1 (2009): 11–21.
[30] L. Min, Y. Yin, Q. Zhao, and S. Wang, "Establishment of a Human iPSC Line (SUTCMi001-A) Derived From a Healthy Donor," *Stem Cell Research* 63 (2022): 102849.
[31] S. Sullivan, G. N. Stacey, C. Akazawa, et al., "Quality Control Guidelines for Clinical-Grade Human Induced Pluripotent Stem Cell Lines," *Regenerative Medicine* 13, no. 7 (2018): 859–866.